Vital Sign Detection Using a Thermal Camera

Zinan Guo, University of Twente, The Netherlands

Animal health monitoring is one of the most critical topics in research nowadays, and by measuring the heart rate and the respiration rate, the welfare of animals could be ensured. However, measuring by wearable sensors could bring stress to animals, and it is not convenient to wear them on animals. In this research, measurements are done in a contactless way by using a thermal camera to record different body parts of calves, and several signal processing methods were used to extract the corresponding respiration rate and heart rate.

Key Words: Calves, Thermal Camera, Heart Rate, Respiration Rate, KCF, FFT.

1 INTRODUCTION

The cow is one of the most important animals on earth [22]. Female calves contribute to dairy production, including milk and cheese, which are crucial for humans. Male calves are essential for beef production, which is quite an important part of human consumption [2]. Besides that, cows can be used to help with agricultural work, which is an essential part of human life. Thus, it is crucial for humans to maintain the high welfare of calves by monitoring their health regularly [8].

To ensure the health and well-being of calves, humans need to monitor their vital signs regularly, including heart rate and respiration rate. Mammals need the circulatory and respiratory systems, two of the most essential systems, to maintain vital signs [7]. These rates together are used to control the metabolic energy production in the body. The information in these two rates can let us know whether the calves are in a comfortable environment and whether their growth, stress level and overall healthiness are at an average level. So heart and respiratory rates contain a lot of health information for mammals. Effective monitoring of the vital signs could also help identify diseases in the early phase to give the calves optimal growth and potentially reduce the farmers' financial loss [6,9].

However, most vital measurements are based on wearable sensors, such as heart-rate monitors. Wearing these devices can cause stress to humans, leading to inaccurate measurements. This drawback might be applied to calves as well. Since wearable sensors are not explicitly designed for calves, they would have the possibility of being broken by the calves while they are playing. Buying these types of equipment can be costly for farmers too.

TScIT 39, July 7, 2023, Enschede, The Netherlands

In recent years, with the maturity of remote detection technology, remote detection devices have been widely used in commercial and scientific research [13,23,24]. In animal health monitoring, remote detection is potentially a better way to monitor health and detect vital signs compared with traditional way of detection for several reasons. One of the most important reasons is that contactless measurement can reduce the stress on the animals, maintaining the welfare of the animals to make them maintain productivity. Another reason is that in the past, people had to use a wearable sensor to do the detection because there did not exist an advanced image processing method to analyse the video file. With the development of image and signal processing technology, people can get more relevant information than before, which can be used as ground truth values.

As a representative example of remote detection equipment, the thermal camera is an excellent choice for detecting vital signs [4,21]. Thermal imaging technology has become more and more mature in recent years. Compared to the big and unmoveable machines in the past, nowadays, we can record thermal videos easily by connecting the thermal camera to our phone. The resolution of the thermal images and videos improved significantly, making analysing the information in the images or videos more accessible [10]. Recent studies showed the potential of estimating heart rate and respiration rate using thermal videos, as shown in the related work section.

After applying several signal processing methods on the relative temperature values, we could know the well-being status of the calf. If the temperature shown by the thermal camera is not in the average fluctuation range, then the status of the calf is not normal, and we can inform the farmer to take measures to reduce their loss. Other researchers have done several related research, including using thermal cameras to detect the heart and respiration rates of humans, pigs and cows [17,18]. However, the field of health monitoring for the calf is still undiscovered, so this paper can fill the blank of the calf monitoring field.

2 RELATED WORKS

Currently, most of the related work is done to detect human heart and respiration rates. Among these, some of the works are done with the help of standard cameras. Several researchers explored the possibility of using a web camera to detect the heart rate of humans [16]. They used Eulerian Video Magnification to do the image analysis, and their result showed that this method is feasible. In the meantime, since the thermal image contains relative temperature values when the normal RGB images do not, thermal cameras are becoming more and more popular when people want to estimate the heart rate and respiration rate. Several researchers used thermal cameras to detect the

respiration rate of cyclists [3]. They settled their camera on a pan-tilt unit and set the region of interest (ROI) to the nose area of the cyclists with the help of the Kullback-Leibler distance (KLD) tracking algorithm. Other researchers used thermal cameras to monitor both the heart rate and respiration rate of humans [5]. They extracted the human face by analysing the temperature value, then set 68 facial landmarks using face pose estimation to settle the ROI.

Since it is vital to ensure the welfare and health of newborn babies, several people used thermal cameras to estimate the respiration rate of newborn infants as well. In a study regarding neonates, standard cameras are used to track the ROI with the help of deep-learning methods [15]. They use a registration algorithm to combine the ROI gathered from standard cameras with thermal cameras to extract the temperature information. In another paper, a brand-new algorithm was developed [19]. Rather than tracking by facial landmarks used by most of the papers, they used a black box approach to keep tracking the ROI by analysing the performance value of the respiration rate signal of each grid in the videos. They also created a dataset containing thermal images and the ground truth for researchers.

Although animal welfare is becoming more and more important these days, the heart rate and respiration rate estimation of animals have yet to be widely explored, and only a few measurements are done with limited kinds of animals. In this paper, several computer vision techniques were used to estimate the cattle's heart rate and respiration rate [12]. For the respiration rate, they used the nose area as the ROI, and for the heart rate, they used Eye, forehead and face as the ROI. They used several pattern recognition techniques to determine the feature points inside the ROI for each of the videos. Then these points were tracked by a modified Kanade-Lucas-Tomasi tracking algorithm (KLT) over each frame in the video. After this, the new ROI was extracted by binary masks. They used the changes of average pixel value inside the ROI to estimate the respiration rate and changes in the brightness of the green colour channel to estimate the heart rate, with the help of several signal processing techniques, including a second-order Butterworth bandpass filter and fast Fourier transform (FFT) to the signals from RGB and thermal videos. In the end, they used Pearson Correlation Coefficient and the p-value to evaluate their result.

The heart rate and respiration rate measurements of pigs are measured by some researchers as well [18]. They only used the chest area as the ROI and used the video of the chest cavity (up and down of the chest caused by the breath and the heart pump) to extract the heart rate and the respiration rate. The feature points are selected automatically by the Shi Tomasi corner detection algorithm. Then these points are tracked by the KLT algorithm. After the relative chest horizontal movement of these points is eliminated by principal component analysis, hamming windowed and zero padding are used before applying FFT to these signals.

3 MEASUREMENT SETUP

The measurement is done over three days on a small local farm near Enschede. The vital signs of four calves which are all less than three months old have been tested. They were put in the small stalls separately to reduce the possible movement of the calf, as shown in Figure 1.

Fig. 1. Calf in the stall.

The thermal videos are recorded using a Seek Thermal Compact Pro. This camera is a portable camera which needs to connect to a phone to use. It has a resolution of 320 x 240, the output frame rate of this camera is less than 9Hz, and the thermal sensitivity is under 70 mK. Thanks to the 32-degree field of view, the videos can be recorded easily without getting too close to the calf, which could cause stress to them.

All the videos are recorded with an observer holding a phone in hand, and the distance between the camera and the calf is within 1m. The steady state of the camera and the distance between the camera and the calf are well controlled by the recorder. Comparing connecting the phone to a fixed phone stand, this method allows us to follow the movement of the calf and to keep the region of interest inside the videos all the time. Considering that this might add unnecessary noise to the video, two different trackers were implemented in this study to overcome this flaw. All steps in the experiment are well considered to maximise the quality of the videos and to make sure that the videos are consistent for analysing.

The length of each video for the respiration rate is 30 seconds. The ground truth of the respiration rate is recorded by visual observation. For part of the thermal videos of the respiration rate, there would exist a parallel video that contains the recording of the movement of the calf's chest. Then the ground truth of the respiration rate is counted manually. The ground truth of the remaining videos is counted directly at the farm.

The length of each video for the heart rate is 20 seconds. The ground truth of the heart rate is measured by the polar wearlink strap. First, the electrode area of the strap is wet to make sure it can fit tightly to the calf's body. Then, the strap is tied to the chest area of the calf, which is the closest area to the calf's heart. The electrode area on the calf is shaved to make sure that the belt can be tight close to the skin to make the measurement more

accurate. This polar wearlink strap has been used in related work regarding cattle, and the accuracy has been validated, shows that the polar wearlink can work well with calves as well due to the only difference in size [14].

4 METHODOLOGY

4.1 Image format

All the objects that are above absolute zero degrees would emit infrared radiation. The higher the temperature, the more radiation would be emitted by the object. This radiation could reflect the relative temperature values, and by detecting the radiation, thermal cameras are able to record thermal videos and create thermal images. The inhale and exhale would bring temperature changes around the nose area, and the minor temperature changes of vessels would reflect the pump of the heart, which makes the thermal images an excellent choice to detect the respiration rate and the heart rate. The colour map used by the thermal camera is needed to map the pixel intensity of a thermal image to the temperature value. Unfortunately, the thermal camera used in this study does not have the functionality to output the colour map, so the absolute temperature in the thermal images is unknown. However, to extract the vital signs, only the temperature changes are essential, so by focusing on the changes of pixel values over time, the corresponding respiration rate and heart rate could still be extracted.

4.2 Region of interest

The next step is to choose the region of interest (ROI). ROI is a subset of data grids in images or videos that is valuable for the researcher, while the other parts of the data grids are not. So by setting the ROI, we could reduce the noise caused by unnecessary information and only do the analysis on the valuable part. For the respiration rate estimation, the ROI is chosen for the nose area of the calf. When inhaling and exhaling, the air around the nose area should have obvious temperature changes, so by analysing the pixel intensity around the nose area, we would get information of the respiration rate. To achieve this, the face of the calf is recorded from the front and the side for the respiration rate analysis.

It is challenging to choose the ROI for the heart rate. The conclusion in a paper shows that the forehead of cattle does have the highest association not only with rectal temperature but also with the temperature-humidity index (THI) [20]. The vessels in the forehead are closer to the skin than other areas, so these areas might show a more robust pattern of the pumps of the heart. Except for the forehead, the hoof, eye, and ear are selected to explore whether other parts of the calf are suitable for estimating the heart rate as well, so during the data collection process, the videos of the forehead area, hoof area, eye area and ear area are recorded.

4.3 Tracker

In each of the videos, the ROI is chosen manually in the first frame. However, it is impossible to choose ROI manually for each frame, this means a tracker is needed to keep tracking where the original ROI is in each of the frames. To achieve that, two different tracking methods are used in the research process, and they are Kernelised Correlation Filters (KCF) tracking algorithm and Kanade-Lucas-Tomasi tracking algorithm (KLT).

KCF is used due to its outstanding tracking performance. Correlation filters are a set of classifiers that are specifically trained to separate the object and the background, which is useful for object tracking [1]. These classifiers are trained by features extracted with the ROI, then used for detecting the ROI in the later frames. However, the original implementation of correlation filters is not sufficient to handle the non-linear data. In 2015, KCF was introduced by Henriques et al. [11]. Compared with the original correlation filter, like some of the machine learning techniques, they mapped the data into higher dimensional feature space. By doing this, the processing speed for the non-linear data is highly improved without losing accuracy. In the implementation, the ROI is selected manually in the first frame of the video. After this, the first frame and the position of the ROI are fed into the tracker. After updating a new frame into the tracker, it would output the position of the ROI in the new frame.

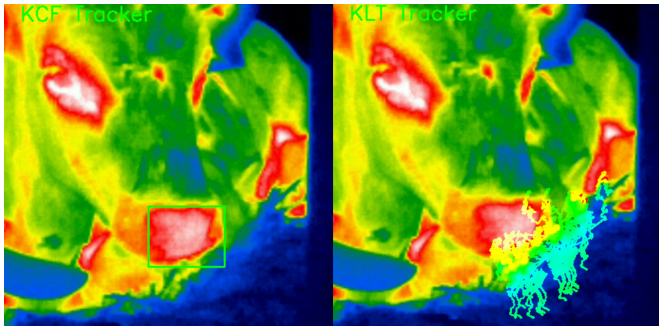

Fig. 2. Tracking process of two different trackers.

The KLT algorithm is used more frequently in the related works and is more understandable compared with KCF. First, the Shi Tomasi corner detection algorithm would automatically choose the best 100 feature points in the ROI. These points are usually the corners in the image which usually have more features than the normal points, so the tracker would be easier to track them among different frames. The KLT algorithm would track the points based on two assumptions. First is that the pixel intensity of the feature points are fixed. Second is that the movement of the neighbours of feature points would be the same as the feature points. By taking these two assumptions into consideration, the KLT algorithm would keep tracking the feature points very sufficiently. An outlier-removing method based on Euclidean distance is implemented and used to remove the outliers due to the tracking error. Since the KLT algorithm could only trace feature points rather than the whole area of the ROI, the ROI would be reset manually according to the coordinates of the new points obtained for each frame after removing the outliers.

However, since the image format used in this study is thermal videos, the corner detection algorithm could not choose the points that could best represent the ROI. The outliers generated

by KLT are also far more than acceptable. Even though the outlier removing method is implemented, if the threshold is set too large then the area of the ROI would be not consistent. If the threshold is set too low, then there won't be enough points to track and to rebuild the ROI during the tracking process. It can be seen easily from the KLT tracking result in Figure 2 that some of its points in the top right corner of the nose area failed tracking, so at the end of the research process, this tracking algorithm was abandoned, and the result is only analysed based on KCF tracking method.

4.4 Signal processing methods

Two different signal processing methods are used in this research. For method 1, while tracking the ROI for each frame, the average pixel intensity is extracted for the whole area of ROI in each frame and stored in a list. Since the time gap between each value is fixed because the fps of the video is 15 at constant, these values could be analysed by FFT directly. However, before analysing this time series data by FFT, two signal preprocessing methods are used to increase the length of the signals and reduce the noise. The second-order Butterworth bandpass filter is used to filter out the frequencies that are outside the interest range. According to the data that we gathered, for the respiration rate, the lower cut and the higher cut are set to 0.33Hz and 1.33Hz, respectively. For heart rate, the lower and high cuts are set to 1.667Hz and 3Hz, respectively. Then zero padding is used to increase the length of the pixel intensity list extracted in the previous step. By adding zeros to the end of the list, the length of the frequencies list output by the FFT would be larger without interfering with the pattern for the original signal, which could result in a more closely spaced frequency. In the code, the signal is padded to a length of 2048. Finally, the FFT would transfer this time-domain data into the frequency-domain. The input of the FFT is the list of pixel intensities over time, and then the output would be all the frequencies and corresponding magnitudes. After taking the absolute value for all the magnitudes, the frequency with the highest magnitude within the cut range would be extracted as the dominant frequency, representing the corresponding respiration rate or the heart rate.

For method 2, rather than analysing based on the average pixel intensity in the whole area of ROI, this method focus on the pixel intensity changes for each of the pixels. After applying the Butterworth filter, zero padding and FFT, the frequency with the maximum magnitude is extracted for every pixel. Later, within the top 10 pixels that have the highest magnitude, the most occurrence frequency would be extracted as the dominant frequency, representing the corresponding respiration rate or the heart rate.

5 RESULTS

For the result of each ROI, several analytical metrics are calculated. Pearson correlation coefficient (r) represents how strong the linear relationship is between the estimated rates and the ground truth. If r is close to 1, then it represents a strong positive relationship, which means that the estimated rate closely follows the ground truth value. R close to 0 and smaller than 0 represents a weak relationship and negative relationship, respectively, both means the estimated rates can not accurately capture the temperature changes caused by respiration or heart pump in the ROI. The P-value refers to the possibility that the correlation above is generated randomly. If the P-value is lower than 0.05, then the null hypothesis could be rejected, meaning that it is quite unlikely that the observed correlation is generated at random. Mean absolute percentage error (MAPE) represents the relative error between the estimated rate and the ground truth, which allows us to compare the accuracy of two different processing methods used in the research.

For the result of the respiration rate assessment, as shown in Table 1, we can see that both methods showed a high correlation with $r > 0.95$ and $p < 0.01$. This means that both signal processing methods have the ability to extract the changes in pixel intensities that correspond to the respiration rate from thermal videos. From the MAPE we can tell that the result generated by the second method is slightly better than the first method. Figure 3 is an example of correlation plot of the result generated by method 2 for the nose area.

Table 1. Result of respiration rates

Analysed Area	Method	Sample size	Pearson correlation coefficients (r)	P-value	Mean Absolute Percentage Error (MAPE)
Nose	1	26	0.984	<0.01	5.80%
Nose	2	26	0.990	<0.01	4.65%

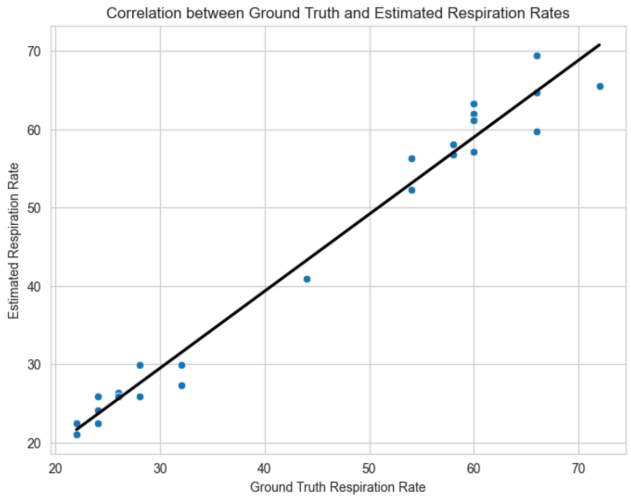


```
Pearson Correlation Coefficient (r): 0.9897609254694307
P-value: 8.320971150543781e-22
MAPE: 4.646568962847557%
```

Fig. 3. Correlation plot between the estimated respiration rate and the ground truth of nose area.

Compared to the result of the respiration rate, the accuracy of the heart rate estimation is pretty low. As shown in Table 2, only the forehead area shows a high correlation between the

estimated rate and the ground truth for both methods with r > 0.5 and p < 0.01, and from MAPE we can tell that the result generated by the second method is better than the first method as well. Although the result for the ear area generated by method 1 shows that the ear area could potentially reflect the heart rate, it is still questionable since the result from method 2 shows a negative linear relationship between the estimated heart rate and the ground truth. The results of the eye and the hoof show that these regions do not represent the actual heart rate with all correlation value less than 0.3, which means the temperature changes in these areas could not reflect the temperature changes caused by the heart pump. Figure 4 is another example of correlation plot of the result generated by method 2 for the forehead area.

Table 2. Result of heart rates

Analysed Area	Method	Sample Size	Pearson correlation coefficients (r)	P-value	Mean Absolute Percentage Error (MAPE)
Forehead	1	24	0.568	<0.01	8.79%
Forehead	2	24	0.613	<0.01	5.61%
Ear	1	15	0.558	<0.05	7.43%
Ear	2	15	-0.400	>0.05	10.82%
Eye	1	19	-0.520	<0.05	15.46%
Eye	2	19	-0.051	>0.05	9.30%
Hoof	1	28	-0.074	>0.05	9.90%
Hoof	2	28	0.215	>0.05	10.61%

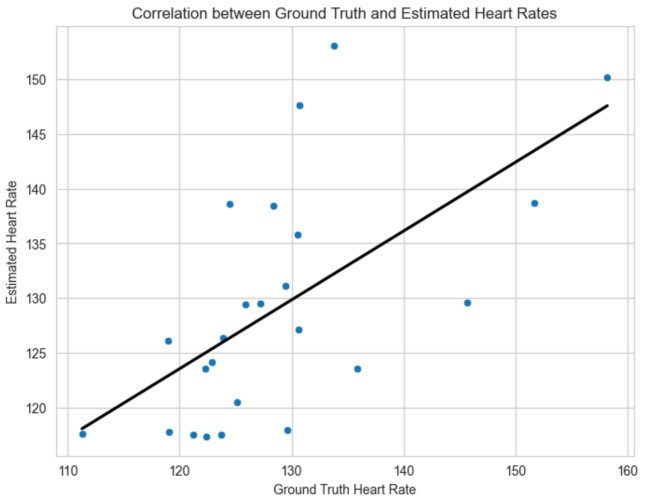

Fig. 4. Correlation plot between the estimated heart rate and the ground truth generated by method 2 for forehead area.

6 DISCUSSION

Currently, the tracking method used in this research is only based on pure computer vision technique. Since the average pixel intensity also considered the noise, while the magnitude of the "noise pixel" is not as high as the pixel which represent the frequency of respiration and heart pump, this might be the reason why the accuracy of the second method is higher than the first method for the nose area and the forehead area. However, if the tracking performance is not good due to lots of movement of the calf, then for the second method, the pixels that have the same coordinates within the ROI between two consecutive frames would not be consistent, which could make the accuracy significantly lower. For the nose and the forehead area, since there does not exist too much movement of the calf in the video, the result generated by the second method is better than the first method. However, the video of the ear area contains much more movement compared with the forehead and the nose area, which leads to very low accuracy for method 2. In the research process, since the ROI is selected manually for each of the videos, this could also lead to minor differences in the results. Thanks to the advanced technology these days, several tracking methods based on artificial intelligence and machine learning have shown incredible performance. There is no tracking method that is specifically designed to track different parts of the calf, but it is doable to train a classifier for this. Although it might be time-consuming, this could potentially result in a higher tracking performance than the normal computer vision methods, improve the accuracy for the second signal processing method used in this research, and would make it possible to modify the whole process into a real-time estimation system.

In several similar studies, the movement of test subjects is well controlled. When the test subjects are human, it is easy to let the test subject remain stable, which is essential for reducing the noise. When the test subjects are calves, things could get out of control. In one of the papers, the researchers put the cattle into a crush, which could reduce the enormous movement of calves, but cattle could still move here and there inside the crush [12]. Unfortunately, the farm where the measurement took place did not have large equipment like the crush. So the only solution is to put the calves into a small stall, as shown in Figure 1. Although calves could not get out of the stall, it is still possible for them to move around inside the stall. It was so tricky when recording the video of several ROI of the calves since it is impossible to let the calf become stable all the time. In the stall, it is also impossible to use a phone stand to reduce the camera's vibration. Since the accuracy of the result of the heart rate highly depends on how much noise there is in the data, these factors may influence the final result to a certain extent.

For the analysis of heart rate, the ideal temperature value changes shown in the pixels should reflect the blood pump circulation. This means that this analysis is highly dependent on the resolution of the thermal camera and the total amount of frames of the video. However, compared with several related works, the camera's resolution, sensitivity, and accuracy of the pixel intensity captured by the camera are significantly smaller than theirs', so this could have a significant impact on the

analysis of the heart rate [12,18]. This is one of the possible reasons that the accuracy of heart rate estimation is significantly lower than the respiration rate. Another possible reason is that the total video length is too short for the stable analysis due to the limited time visited the farm. If the number and the length of videos of the heart rate could be much more than current data, it may lead to a better result as well.

7 CONCLUSION

In this paper, we proposed a non-invasive way to estimate the respiration rate and the heart rate of the calf. After extracting the pixel intensities in the thermal video of different parts of the calf, the heart rate and respiration rate would be represented by the dominant frequency that has the highest magnitude. We showed that the accuracy is promising by choosing the ROI as the nose area of the calf for the respiration rate, and the forehead area for the heart rate. Although the result of the forehead outweighs the hoof, eye and ear area, in all, the performance could be significantly better if more advanced thermal cameras and tracking methods were used or with the help of a crush in the measurement process. For future work, as shown by the high accuracy of the respiration rate and the heart rate for the forehead area, after changing the tracker into a real-time tracking system, this pipeline could be applied in a real-time vital signs estimation system using a thermal camera.

REFERENCES

[1] Vishnu Naresh Boddeti. 2012. Advances in correlation filters: vector features, structured prediction and shape alignment. phd. Carnegie Mellon University, USA.

[2] Donald M. Broom. 2021. A method for assessing sustainability, with beef production as an example. Biological Reviews 96, 5 (2021), 1836–1853. DOI:https://doi.org/10.1111/brv.12726

[3] Ronan Chauvin, Mathieu Hamel, Simon Brière, François Ferland, François Grondin, Dominic Létourneau, Michel Tousignant, and François Michaud. 2016. Contact-Free Respiration Rate Monitoring Using a Pan–Tilt Thermal Camera for Stationary Bike Telerehabilitation Sessions. IEEE Systems Journal 10, 3 (September 2016), 1046–1055. DOI:https://doi.org/10.1109/JSYST.2014.2336372

[4] De-Ming Chian, Chao-Kai Wen, Chang-Jen Wang, Ming-Huan Hsu, and Fu-Kang Wang. 2022. Vital Signs Identification System With Doppler Radars and Thermal Camera. IEEE Transactions on Biomedical Circuits and Systems 16, 1 (February 2022), 153–167. DOI:https://doi.org/10.1109/TBCAS.2022.3147827

[5] S. Coşar, Z. Yan, F. Zhao, T. Lambrou, S. Yue, and N. Bellotto. 2018. Thermal Camera Based Physiological Monitoring with an Assistive Robot. In 2018 40th Annual International Conference of the IEEE Engineering in Medicine and Biology Society (EMBC), 5010–5013. DOI:https://doi.org/10.1109/EMBC.2018.8513201

[6] Juan V. Durá, Giuseppe Caprara, Marco Cavallaro, Andrea Ballarino, Christian Kaiser, and Dieter Stellmach. 2014. New technologies for the flexible and eco-efficient production of customized products for people with special necessities: Results of the FASHION-ABLE project. In 2014 International Conference on Engineering, Technology and Innovation (ICE), 1–7. DOI:https://doi.org/10.1109/ICE.2014.6871558

[7] Malcolm Elliott and Alysia Coventry. 2012. Critical care: the eight vital signs of patient monitoring. Br J Nurs 21, 10 (May 2012), 621–625. DOI:https://doi.org/10.12968/bjon.2012.21.10.621

[8] European Commission. Directorate General for Health and Food Safety. and TNS Political & Social. 2015. Attitudes of Europeans towards animal welfare: report. Publications Office, LU. Retrieved May 2, 2023 from https://data.europa.eu/doi/10.2875/884639

[9] Nicolas Farina, Gina Sherlock, Serena Thomas, Ruth G. Lowry, and Sube Banerjee. 2019. Acceptability and feasibility of wearing activity monitors in community-dwelling older adults with dementia. International Journal of Geriatric Psychiatry 34, 4 (2019), 617–624. DOI:https://doi.org/10.1002/gps.5064

[10] Rikke Gade and Thomas B. Moeslund. 2014. Thermal cameras and applications: a survey. Machine Vision and Applications 25, 1 (January 2014), 245–262. DOI:https://doi.org/10.1007/s00138-013-0570-5

[11] João F. Henriques, Rui Caseiro, Pedro Martins, and Jorge Batista. 2015. High-Speed Tracking with Kernelized Correlation Filters. IEEE Trans. Pattern Anal. Mach. Intell. 37, 3 (March 2015), 583–596. DOI:https://doi.org/10.1109/TPAMI.2014.2345390

[12] Maria Jorquera-Chavez, Sigfredo Fuentes, Frank R. Dunshea, Robyn D. Warner, Tomas Poblete, and Ellen C. Jongman. 2019. Modelling and Validation of Computer Vision Techniques to Assess Heart Rate, Eye Temperature, Ear-Base Temperature and Respiration Rate in Cattle. Animals (Basel) 9, 12 (December 2019), 1089. DOI:https://doi.org/10.3390/ani9121089

[13] Depan Lian. 2021. Remote detection method of concrete bridge surface cracks based on digital image. In International Conference on Smart Transportation and City Engineering 2021, SPIE, 1516–1521. DOI:https://doi.org/10.1117/12.2615591

[14] Janzekovic Marjan, B. Muršec, and Ignac Janžekovič. 2006. Techniques of measuring heart rate in cattle. Technical Gazette; Vol.13 No.1,2 13, (January 2006).

[15] Lalit Maurya, Reyer Zwiggelaar, Deepak Chawla, and Prasant Mahapatra. 2022. Non-contact respiratory rate monitoring using thermal and visible imaging: a pilot study on neonates. J Clin Monit Comput (December 2022). DOI:https://doi.org/10.1007/s10877-022-00945-8

[16] Nadica Miljkovic and Dragan Trifunović. 2014. Pulse rate assessment: Eulerian Video Magnification vs. electrocardiography recordings. DOI:https://doi.org/10.1109/NEUREL.2014.7011447

[17] Luwei Nie, Daniel Berckmans, Chaoyuan Wang, and Baoming Li. 2020. Is Continuous Heart Rate Monitoring of Livestock a Dream or Is It Realistic? A Review. Sensors 20, 8 (January 2020), 2291. DOI:https://doi.org/10.3390/s20082291

[18] Carina Barbosa Pereira, Henriette Dohmeier, Janosch Kunczik, Nadine Hochhausen, René Tolba, and Michael Czaplik. 2019. Contactless monitoring of heart and respiratory rate in anesthetized pigs using infrared thermography. PLOS ONE 14, 11 (November 2019),

e0224747.
DOI:https://doi.org/10.1371/journal.pone.0224747

[19] Carina Barbosa Pereira, Xinchi Yu, Tom Goos, Irwin Reiss, Thorsten Orlikowsky, Konrad Heimann, Boudewijn Venema, Vladimir Blazek, Steffen Leonhardt, and Daniel Teichmann. 2019. Noncontact Monitoring of Respiratory Rate in Newborn Infants Using Thermal Imaging. IEEE Transactions on Biomedical Engineering 66, 4 (April 2019), 1105–1114.
DOI:https://doi.org/10.1109/TBME.2018.2866878

[20] Marcia Saladini Vieira Salles, Suelen Corrêa da Silva, Fernando André Salles, Luiz Carlos Roma, Lenira El Faro, Priscilla Ayleen Bustos Mac Lean, Celso Eduardo Lins de Oliveira, and Luciane Silva Martello. 2016. Mapping the body surface temperature of cattle by infrared thermography. Journal of Thermal Biology 62, (December 2016), 63–69.
DOI:https://doi.org/10.1016/j.jtherbio.2016.10.003

[21] Guanghao Sun, Yosuke Nakayama, Sumiyakhand Dagdanpurev, Shigeto Abe, Hidekazu Nishimura, Tetsuo Kirimoto, and Takemi Matsui. 2017. Remote sensing of multiple vital signs using a CMOS camera-equipped infrared thermography system and its clinical application in rapidly screening patients with suspected infectious diseases. Int J Infect Dis 55, (February 2017), 113–117.
DOI:https://doi.org/10.1016/j.ijid.2017.01.007

[22] Stanley W. Trimble and Alexandra C. Mendel. 1995. The cow as a geomorphic agent — A critical review. Geomorphology 13, 1 (September 1995), 233–253.
DOI:https://doi.org/10.1016/0169-555X(95)00028-4

[23] Dongyang Xie, Jun Cheng, and Dapeng Tao. 2019. A New Remote Sensing Image Dataset for Large-Scale Remote Sensing Detection. In 2019 IEEE International Conference on Real-time Computing and Robotics (RCAR), 153–157.
DOI:https://doi.org/10.1109/RCAR47638.2019.9043971

[24] 2021. APPLICATION OF COMPUTER NETWORK VIRTUAL INSTRUMENT TECHNOLOGY IN THE DEVELOPMENT OF A CONSTRUCTION MACHINERY REMOTE DETECTION SYSTEM. IJOMAM 1, 10 (November 2021).
DOI:https://doi.org/10.17683/ijomam/issue10/v1.12